The International Journal of Advanced Manufacturing Technology
https://doi.org/10.1007/s00170-023-11888-y

ORIGINAL ARTICLE

Wafer particle inspection technique using computer vision based on a color space transform model

Heebum Chun[1] · **Jingyan Wang**[1] · **Jungsub Kim**[1] · **ChaBum Lee**[1]

Received: 23 January 2023 / Accepted: 30 June 2023

Abstract
The preparation of defect-free wafers serves as a critical stage prior to fabrication of devices or chips as it is not possible to pattern any devices or chips on a defected wafer. Throughout the semiconductor process, various defects are introduced, including random particles that necessitate accurate identification and control. In order to effectively inspect particles on wafers, this study introduces a wafer particle inspection technique that utilizes computer vision based on HSV (hue-saturation-value) color space transformation models to detect and to classify different particles by types. Artificially generated particle images based on their color properties were used to verify HSV color space models of each particle and to demonstrate how the proposed method efficiently classifies particles by their types with minimum crosstalk. A high-resolution microscope consisting of an imaging system, illumination system, and spectrometer was developed for the experimental validation. Micrometer-scale particles of three different types were randomly placed on the wafers, and the images were collected under the exposed white light illumination. The obtained images were analyzed and segmented by particle types based on pre-developed HSV color space models specified for each particle type. By employing the proposed method, the presence of particles on wafers can be accurately detected and classified. It is expected to inspect and classify various wafer particles in the defect binning process.

Keywords Wafer metrology and inspection · Particle inspection · Color space transform · Hue-saturation-value (HSV)

1 Introduction

The manufacturing of semiconductor devices plays a pivotal role in various technological fields, ranging from electronics, telecommunications, computing, and beyond [1–4]. One of key aspects of semiconductor manufacturing is ensuring the production of defect-free wafers, which form the foundation for device fabrication. However, during the semiconductor process, various defects are introduced that includes systematic defects and random particles [5]. Among the prevailing challenges in the manufacturing process is the presence of particles on the wafer surface, originating from diverse sources such as contamination during handling, processing, or environmental factors [6, 7]. Their sizes can vary from sub-micrometer to larger scales, and their composition can span a wide range of materials. The presence of defects on wafers can significantly impact device performance, functionality, yield, and overall manufacturing costs. Consequently, the implementation of effective inspection techniques is essential for identifying and characterizing defects.

In recent years, computer vision techniques have emerged as a promising approach to address the particle inspection challenges in semiconductor manufacturing, offering automated and efficient methods for defect detection and classification. Additionally, the utilization of color space transformations has shown promising results in enhancing the performance of defect inspection systems. In particular, the HSV (hue, saturation, and value or brightness) color space transform gained significant attention in various image processing applications. The HSV color space model was first introduced in 1978 [8] and has been known as an alternative representation of the RGB (red, green, blue) color model, offering a better colorimetric analysis and perception than the RGB color space model. HSV color transform capture variations in the color type referred to as "hue" that represents true color, varying from red to green and blue. The

✉ ChaBum Lee
cblee@tamu.edu

[1] J. Mike Walker '66 Department of Mechanical Engineering, Texas A&M University, 3123 TAMU, College Station, TX 77843-3123, USA

Published online: 05 July 2023

"saturation" represents the purity of color, while the "value" represents the brightness of the color, in 0–100% scale range [9]. Because the HSV color space model is highly accurate as the way humans perceive colors, it has been widely used in image processing and computer graphics applications since a few decades ago [10]. With the development of advanced algorithms and enhanced computational capabilities enabling fast, accurate, reliable color space conversion between the RGB and HSV models by using digital signal processors (DSPs), the HSV color space models have been used in various applications including human skin detection [11–13], face recognition [14], object tracking [15], defect detection [16, 17], bio- and health condition diagnosis [18, 19], and particle color property identification [20, 21].

The HSV color space transform method has also been recently applied to the field of wafer defect inspection [22–24]. Dangayach et al. employed computer vision techniques and machine learning algorithm, utilizing the HSV color space to detect defects on the Redistribution Layer (RDL) [25]. Kim et al. utilized an image process using HSV color space to inspect different crystalline forms of SiC wafer [26]. Although the methods have potential for defect inspection techniques, the HSV color space has primarily been focused on surface defect classification or large-scale detection, where particle sizes can be as small as a few or sub-micrometers. Other wafer defect measurement methods heavily rely on optics systems [27–29]. Takahashi et al. proposed a novel optical measurement technique capable of nondestructively detecting Si wafer defects with a spatial resolution of 100 nm using infrared standing evanescent wave [30]. Okamoto et al. investigated particle inspection on wafers using UV laser scattering that can achieve the detection of sub-micrometer sized particles [31]. Nevertheless, the performance of methods highly depends on the beam size which restricts the resolution, or the performance can only identify the presence of particles that cannot lead to the further classification of different types of particles. Additionally, in most semiconductor assemblies, the inspection operations are conducted by human experts and thus skilled laborers are required. Competent workers are committed to an inspection, but the integrity of the inspection stage becomes more challenging as the size of defects becomes smaller and more complex [32]. Because manual defect detection based on visual inspection lacks accuracy and is time-consuming which is directly related to the yield rate and manufacturing cost, automated defect inspection is critical in wafer manufacturing processes.

To address limitations and challenges, this study introduces a computer vision-based wafer particle inspection technique using the HSV color space model that not only identifies the presence of particles on the surface of the silicon wafer but also separates and classifies the types of particles while maintaining high-resolution images obtained using a high-resolution microscopic system. The proposed method was both tested analytically and experimentally based on the artificial particle image and experimental images with randomly distributed a few microns of particles on the surface of the silicon wafer. By employing the proposed method, the presence of particles on wafers can be accurately detected and classified. The method enables the classification of undefective or defective wafers that ultimately use for the advanced defect binning process.

2 Method

The proposed wafer particle inspection methods utilize the HSV color space transformation for identifying the presence of particles on the surface of wafers, and the method further characterizes and categorizes the types of particles. Each particle possesses distinct optical properties, such as light transmittance and reflectance. To better capture and analyze these unique properties, HSV color transformation can be utilized instead of solely relying on RGB color analysis. By transforming the RGB color map into HSV, a closer relationship can be established between the optical properties of each particle and their respective HSV representation. The hue component reflects the dominant spectral color observed in the particle, providing valuable information about the material composition or surface characteristics. The saturation component quantifies the purity of the observed color, indicating the degree of dominance of that particular color in relation to other colors present. Lastly, the value component represents the brightness or intensity of the color, shedding light on the overall reflectance or transmittance properties of the particle. These components collectively enable a more comprehensive understanding of the optical behavior of different types of particles. Hence, as optical properties vary among different particles, types of particles can be classified with their unique HSV representations or models.

Figure 1 details the flowchart of the particle inspection image process. The process is mainly divided into two steps: image pre-processing and implementation of the pre-defined HSV model. The process starts with the comparison between the background image which is the image without any particles on the wafer and the foreground image with particles for background removal and particle image extraction. The intensity of each pixel in the back and foreground images can be one-to-one compared in a converted grayscale image. $F_{i,j}$, $B_{i,j}$, and $M_{i,j}$ denote the foreground, background, and mask image intensities, respectively. If the intensities of the foreground and background image are not identical, the mask image will store the intensity of the corresponding pixel as 1 to hold the color of the respective pixel when masking the foreground image, and if they are identical, the intensity of the corresponding mask pixel will be sent to

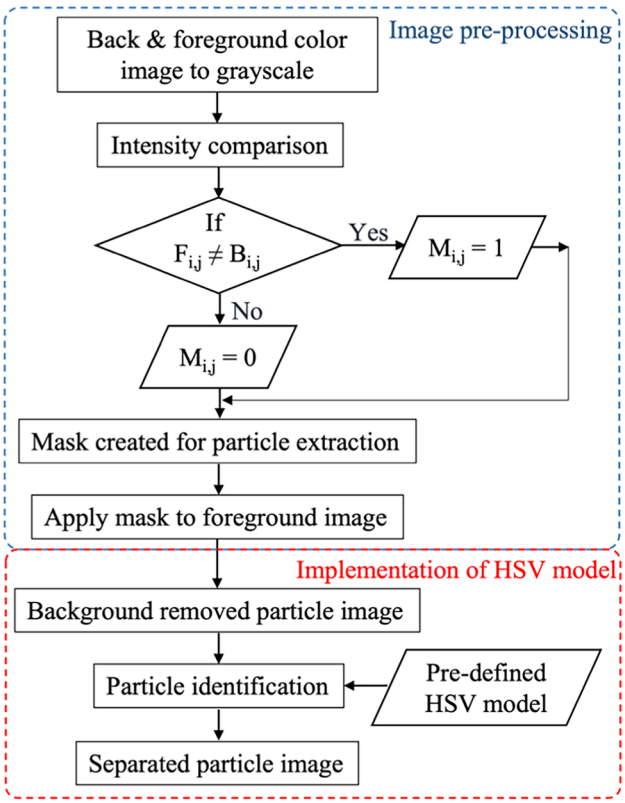

Fig. 1 Image processing flowchart for wafer particle inspection

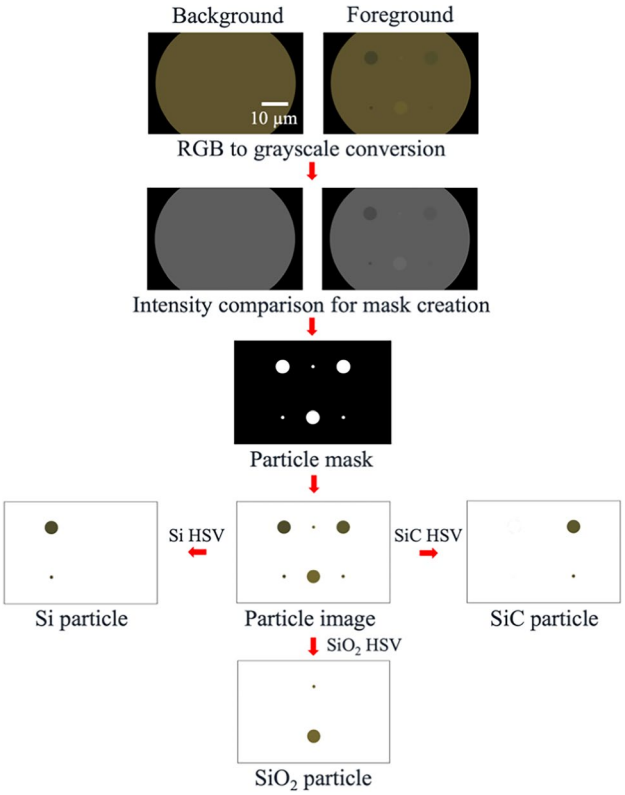

Fig. 2 HSV color transformation model test results with artificial images

zero to remove the background. After creating the mask, it is applied to the foreground image such that the particle image can only be maintained. The following step is to implement the pre-defined HSV color model for particle separation. The particles are separated by using a pre-defined HSV threshold that contains the unique color attributes of each particle. Thus, the final results of images can be segregated by the types of particles with the removed background.

To simulate the proposed method, back and foreground images were artificially generated, and the foreground image contained Si, SiC, and SiO_2 particles as shown in Fig. 2. The scale of artificial image used in this study was the same as the scale of the actual microscope images for ensuring the consistency. Each particle was placed in the foreground image in sizes of 5 μm and 1 μm, and the RGB colors of the background and each particle were selected based on the real images from the microscope. As illustrated with the flowchart, the color images were first converted into grayscale for intensity comparison in each pixel. Based on the intensity comparison, the generated particle mask was applied to the foreground image and the masked image could produce only the particle image as the artificial image does not include the image noise. The black color of the background was simply changed to white for clear visualization after the masking for the particle extraction image. HSV color space models for each particle were pre-determined based on the experiment, and by applying the pre-defined model to the particle-extracted image, different types of particles were able to be separated.

HSV models for Si and SiO_2 particles showed no crosstalk; however, when the SiC HSV model was applied, some crosstalk error was observed, as depicted in Fig. 3. To address this issue, unwanted crosstalk after applying the SiC HSV model was removed by using a widely known morphological transformation operation [33]. Morphological transformation first erodes the image to remove smaller objects or lines with a certain threshold determined based on the evaluation of the pixel area in crosstalk error region where the area was 100 times smaller than the area of smallest 1 μm size particles. Thus, any pixel area that is 100 times smaller than the area of particle size was considered as crosstalk error or image noise and removed from the image. Subsequently, the image was dilated to restore the reduced area caused by eroding. The image mask prepared through morphological transformation was then applied to the original image to remove the crosstalk error. Consequently, the final images after the image pre-processing, implementation of the HSV model, and image post-processing with morphological transformation showed the images with segmented particles only without any interference between the particles

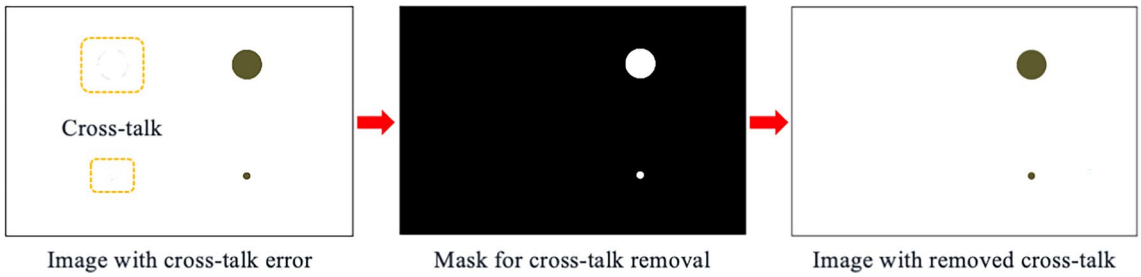

Fig. 3 Morphological transformation for crosstalk removal

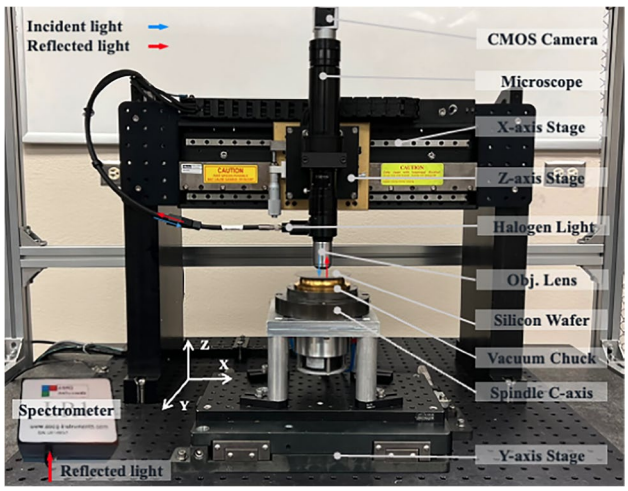

Fig. 4 Wafer particle inspection experimental setup

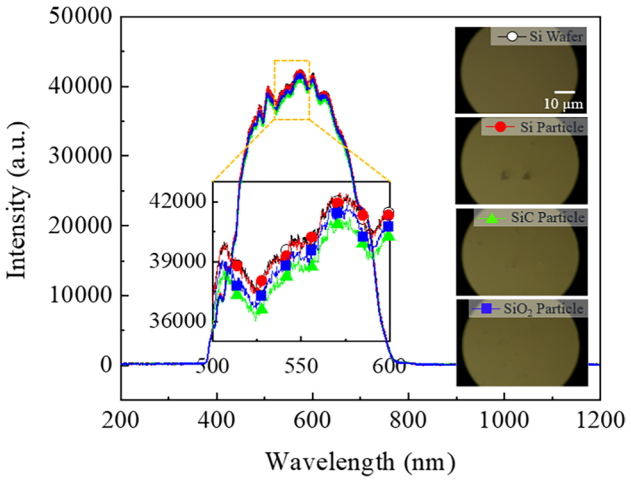

Fig. 5 Spectrometer result of the clean Si wafer surface and the wafer surface with distributed 3 different particles: Si, SiC, and SiO_2

and without background. By maintaining consistent scale between the artificial image and the real microscope images, the morphological transformation on the artificial image could directly extrapolated and applied to the real images, and it was only applied in the case of the SiC model later in the experiment section as crosstalk was not observed in Si and SiO_2 cases.

3 Experiments

For experimental validation, an experimental setup was developed for wafer particle inspection as illustrated in Fig. 4. The wafer scanning system was built with three linear stages (x-, y-, and z-axes) and one spindle axis. A microscope was mounted on the z-axis stage to properly focus the target sample, and X and Y linear stages were implemented for scanning the whole wafer surface. A vacuum chuck on the artifact of the spindle axis can directly hold the wafer. The inspection system includes a high-resolution microscopic system that consists of a 2×1 bifurcated optical fiber, beam splitter, 20-megapixel resolution color CMOS (Complementary Metal-Oxide-Semiconductor) camera, and 100× objective lens with a 4.5× microscope zoom lens. The high-resolution microscopic system utilized in this study has the capability to capture images with field of view (FOV) of 50 μm. The system was also equipped with continuous white light for illumination. When the incident light hits the measurement target, the surface of the wafer, the reflected light can be traveled to the imaging sensor, and using a bifurcated fiber, the reflected light can also be delivered to the installed spectrometer. The high-resolution imaging system can capture small sizes of down to a few micrometers of particles.

Prior to investigating the proposed HSV color space method for particle inspection, 4 cases of spectrometer results were obtained and analyzed where Si Wafer refers to the surface of the clean water without any particles, and Si, SiC, and SiO_2 particles correspond to the randomly distributed individual particle on each surface of the wafer. As shown in Fig. 5, the spectrometer results did not reveal any significant differences among different particle conditions. This lack of differentiation can be attributed to the prominence of the background signal compared to the signals from the particles or the beam size. Consequently, with a spectrometer, it can neither

identify whether there is a presence of particles on the surface of the wafer, nor the types of the particle. Moreover, some particles presented a challenge for visual observation due to their small size and color similarity to the background. To overcome the limitation, this study focuses on machine vision using the HSV color space transformation, which offers the potential to overcome the constraints imposed by visual inspection and conventional measurement methods, allowing for improved detection and classification of small particles.

For an entire experiment, 3 different types of particles, Si, SiC, and SiO_2, were used for the study. Using a high-resolution microscope, a total of 8 different cases of images, including individual particle images, images with 2 mixed particles, images with 3 mixed particles randomly distributed on the surface of the wafer for foreground images, and finally an image of the clean Si wafer without any particles for the background image, were captured. The captured images were used and tested for the experimental validation of the proposed method. The particle inspection approach for the experiment was identical to the simulated study except for the experiment; the bilateral filter was applied before the image pre-processing to minimize the noise in images for an optimal intensity comparison. Additionally, unlike the simulated study which is based on the mono RGB color in features, real images contain variances in the color that causes intensity variations. Thus, instead of using equality comparison in intensity comparison, the foreground and background intensities were compared with ± 2.5% differences between back and foreground images to create the particle mask. Similar to the result of the simulated study, if the foreground image has an intensity difference within ± 2.5% of the background image, created mask had 1 for a corresponding intensity of the pixel. Otherwise, the intensities of the mask had 0 to eliminate the background. After masking the foreground image, the black background color was converted to white for visual clarity. As shown in Fig. 6, after the masking, the particle image contains some unwanted noise because comparing intensity by itself cannot completely remove the image noise. However, after applying the HSV model, which was experimentally found for a corresponding particle, the result provided a clear particle image without the presence of noise or background.

The experimentally determined HSV color models for each specific particle type were converted into a color map, as depicted in Fig. 7, and corresponding HSV color threshold values are listed in Table 1. Although visually distinguishing the individual HSV models was challenging in hue and saturation component due to their similarity, a clear distinction was observed in the degree of the value component in the color map. Upon closer examination

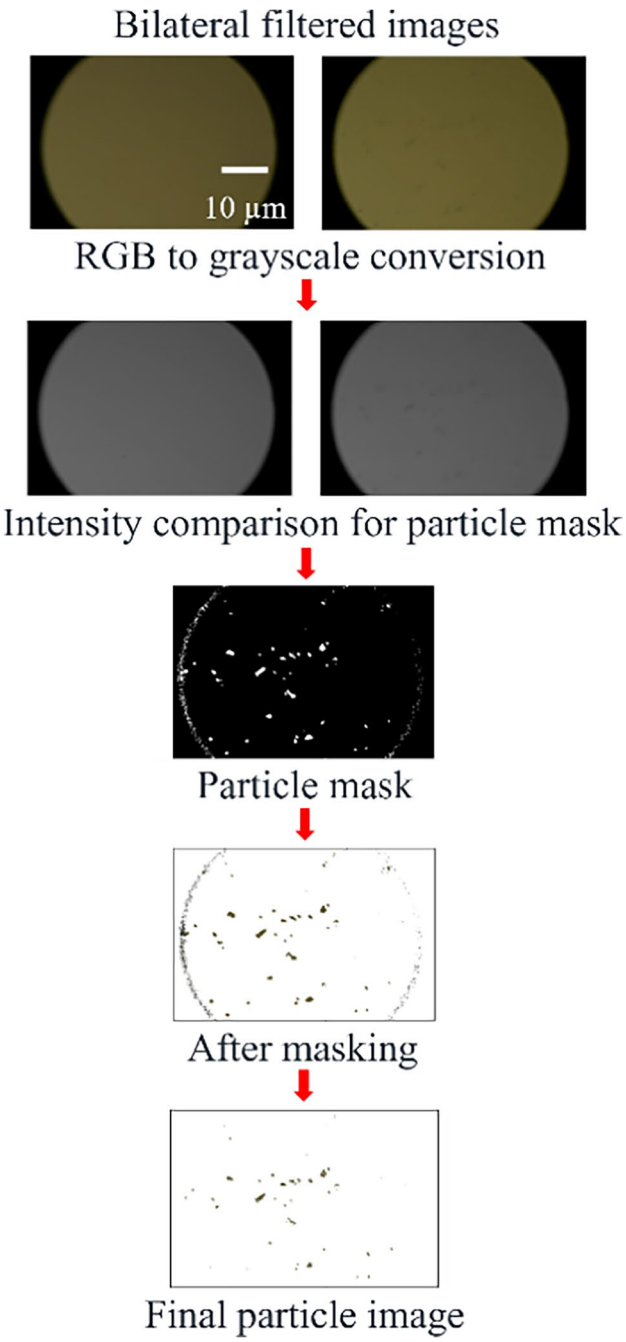

Fig. 6 Wafer particle inspection procedure with an experiment image

of Table 1, the ranges of hue and saturation components overlapped, posing challenges in differentiating particles based on these parameters. However, the value component for each particle type exhibited distinct differences. Consequently, it was observed that the most sensitive and deterministic factor for identifying the different particle types was the value component, which directly correlates with the intensity, lightness, or brightness of the color and is closely related to light absorption.

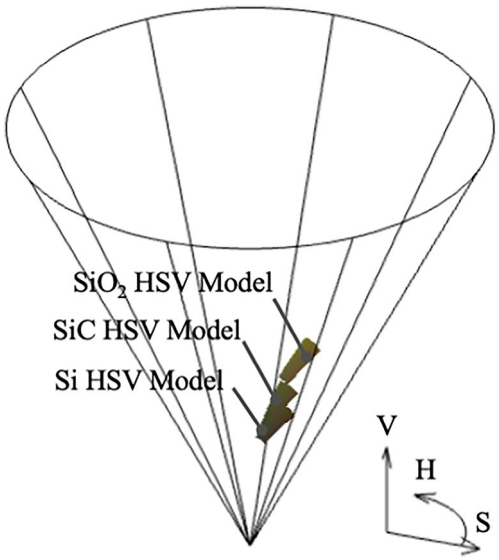

Fig. 7 HSV color map of experimentally determined HSV models

Table 1 Experimentally determined HSV color transformation model of each particle

Particle	Hue	Saturation	Value
Si	[0.083 0.219]	[0.242 0.587]	[0.247 0.303]
SiC	[0.104 0.194]	[0.391 0.571]	[0.304 0.348]
SiO_2	[0.103 0.164]	[0.427 0.669]	[0.376 0.443]

4 Results

Experimentally determined HSV transformation color models for different types of particles were initially applied to the individual particle wafer images before being applied for the mixed particle separation to observe the capability of HSV models in particle detection. Figure 8 illustrates the process of applying HSV models to microscope wafer images. Starting at the top, the original images are comprised of Si particles, SiC particles, and SiO_2 particles only on the surface of the wafer. Mask images for the particle segregation were prepared first by background and foreground image comparison. In contrast to the study using artificial images which gave particle images after the masking, masked images on experimental images included particle images with some image noise due to intensity variations. However, the image comparison could remove most of the background, focusing primarily on the particles. By applying the HSV color models to the masked image, the particle image can be extracted, and the method even eliminates the background which assists to have a clearer visualization of the particle image. Additionally, it had the capability of identifying the presence of a few micrometer particles on the surface of the wafer.

Experimentally developed HSV color models were applied in the mixed particle conditions to validate the capability of method in classifying by their types. On the surface of the wafer, two mixed particles—Si with SiC, Si with SiO_2, and SiC with SiO_2—were randomly dispersed, and the particle inspection procedure was identical to what was mentioned above. After the masking process, each experimentally determined HSV model as listed in Table 1 was applied to the masked image to

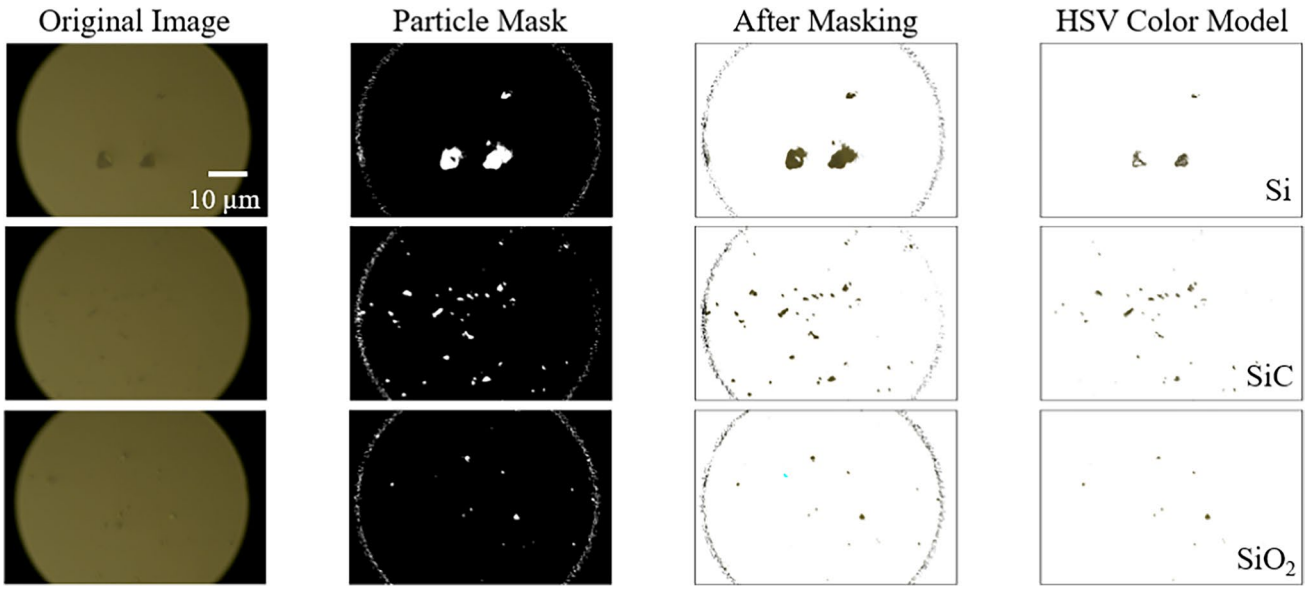

Fig. 8 Each particle image using an experimentally determined HSV color transformation model

differentiate each particle by type. The result of applying the HSV color models to mixed particle images is shown in Fig. 9. The proposed method for wafer particle inspection was successful in distinguishing particles of different sizes. Furthermore, the experimental results showed that when applying different HSV models to the mixed particle images for particle separation, the separated mixed particles were not overlapped and located at different locations. This indicates that the method was effective in classifying and separating mixed particles based on their unique optical characteristics using the developed HSV color models.

Lastly, all three different types of particles used in the study were mixed and randomly distributed on the surface of the wafer. Looking at the original image, while some particles are visible, other particles were indistinguishable from the background and the type of particles is indiscernible by the human vision. However, to the two particles mixed case, by implementing the HSV models, particles could be separated by types, and they were identified at different locations without cross-talk error presented on the final image. Additionally, in line with the results obtained from the simulated study using artificially generated images, the image processing technique using HSV color models could be successfully applied to experimental microscope images which demonstrates the robustness and effectiveness of the proposed method in practical applications for wafer particle inspection. Thus, the proposed method is anticipated to be used on a wafer inspection system for classifying various types of particles in defective wafers for an advanced wafer defect binning process (Fig. 10).

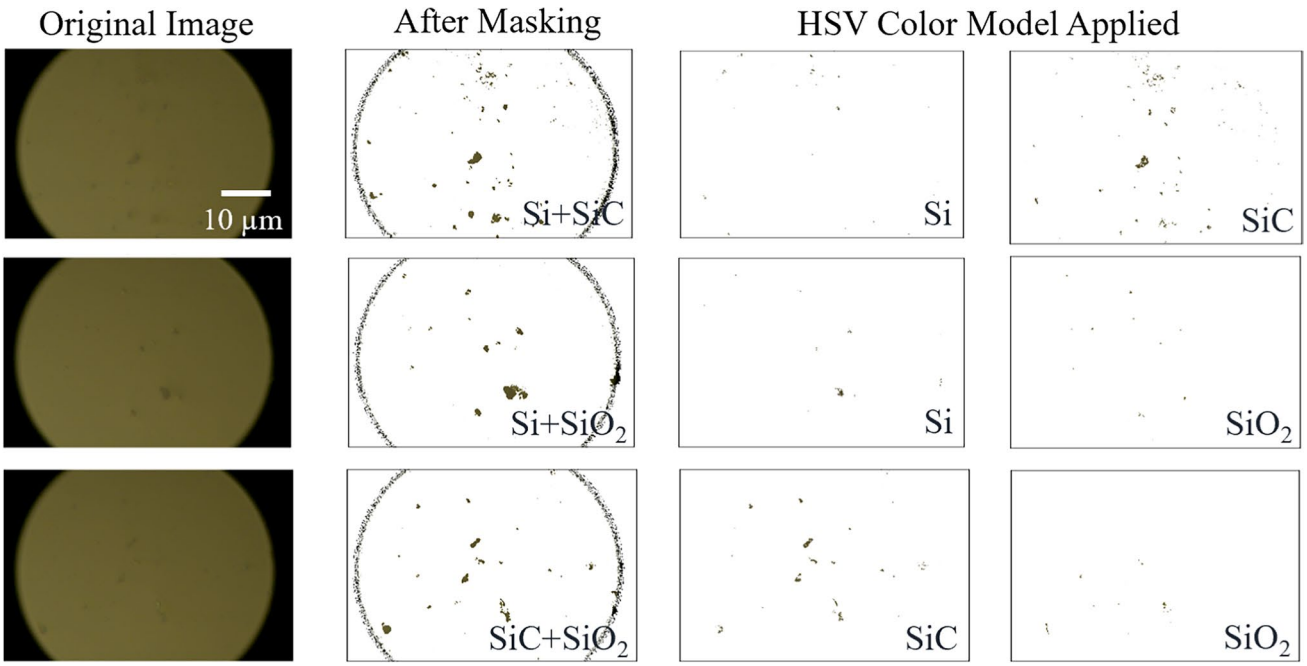

Fig. 9 HSV color transformation models applied in two mixed particle images

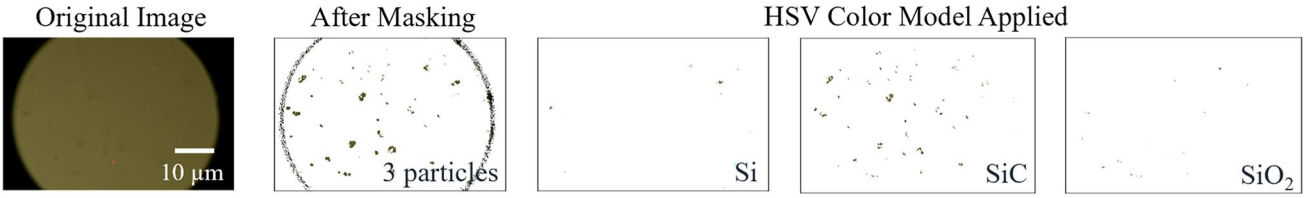

Fig. 10 HSV color transformation models applied in three mixed particle images

5 Conclusion

A novel wafer particle inspection technique based on computer vision was introduced and investigated. First, artificial images were generated and used to test the proposed method, and the results showed that the developed algorithm could detect the micrometer-sized particles on the wafer and further categorize the particles by types based on pre-defined HSV models. Due to the diffraction limit of the objective lens, the micrometer-scale-sized particles were considered in this study. The method was also experimentally validated using a high-resolution microscopy-based wafer inspection system. The spectrometer result showed the incapability of discerning particles on wafers as background image noise was more dominant than the sizes of particles. On the other hand, the proposed method could inspect the wafer surface with minimum crosstalk, and using experimentally defined HSV color space models, the particles could be separated by type. The resulting images were visually clear without crosstalk between the particles and the background. Additionally, the results of the proposed method using experimental images were consistent with those obtained from the simulated study using artificially generated images, demonstrating the robustness and effectiveness of the method in practical applications. The proposed method is simple, fast, and easy-to-use and showed a good particle classification performance. Thus, the method is expected to be utilized in the wafer defect inspection steps, enhancing the wafer defect binning process.

Author contribution All authors equally contributed to this study: design, experiment, and data analysis.

Funding This research has been supported by the National Science Foundation (CMMI #212499).

Data availability The data that support the findings of this study are available from the corresponding author upon reasonable request.

Declarations

Competing interests The authors declare no competing interests.

References

1. Brennan KF, Brown AS (2002) Theory of modern electronic semiconductor devices. John Wiley
2. Lee E-H, Park K (2000) Potential applications of nanoscale semiconductor quantum devices for information and telecommunications technologies. Mater Sci Eng B 74(1–3):1–6. https://doi.org/10.1016/S0921-5107(99)00524-3
3. Nikandish R, Blokhina E, Leipold D, Staszewski RB (2021) Semiconductor quantum computing: toward a CMOS quantum computer on chip. IEEE Nanotechnol Mag 15(6):8–20. https://doi.org/10.1109/MNANO.2021.3113216
4. Ueda H, Sugimoto M, Uesugi T, Kachi T (2006) Wide-bandgap semiconductor devices for automobile applications. GaN 790:1–8
5. Zhu J, Liu J, Xu T, Yuan S, Zhang Z, Jiang H, Honggang G, Zhou R, Liu S Optical wafer defect inspection at the 10 nm technology node and beyond. Int J Extrem Manuf 4:032001. https://doi.org/10.1088/2631-7990/ac64d7
6. Hattori T, Okamoto A, Kuniyasu H (2003) Challenges of finer particle detection on unpatterned silicon wafers, in Characterization and Metrology for ULSI Technology 2003, vol 683. Proc American Inst Physics Conf, Austin, TX, pp 271–277
7. Hattori T (1998) Detection and analysis of particles in production lines, Ultra Clean Surface Processing of Silicon Wafers. Springer-Verlag, New York, pp 243–258
8. Smith AR (1978) Color gamut transform pairs. ACM SIGGRAPH Comp Graph 12(3):12–19
9. Li D (2008) HSV Color Space. In: Encyclopedia of microfluidics and nanofluidics. Springer, Boston, MA. https://doi.org/10.1007/978-0-387-48998-8_656
10. Chernov V, Alander J, Bochko V (2015) Integer-based accurate conversion between RGB and HSV color spaces. Comput Electr Eng 46:328–337. https://doi.org/10.1016/j.compeleceng.2015.08.005
11. Kolkur, Seema, D. Kalbande, P. Shimpi, Chaitanya Bapat and Janvi Jatakia (2017) Human Skin Detection Using RGB, HSV and YCbCr Color Models. ArXiv abs/1708.02694
12. Sahnoune A, Dahmani D, Aouat S (2020) A rule based human skin detection method in CMYK color space. In: International Symposium on Modelling and Implementation of Complex Systems. Cham: Springer International Publishing, pp 233–247
13. Kakumanu PK, Makrogiannis S, Bourbakis NG (2007) A survey of skin-color modeling and detection methods. Pattern Recognit 40:1106–1122
14. Wang SJ, Yang J, Zhang N, Zhou CG (2011) Tensor discriminant color space for face recognition. IEEE Trans Image Process 20(9):2490–2501. https://doi.org/10.1109/TIP.2011.2121084
15. Park JH, Lee GS, Kim JS, Ryu SH, Lee SH (2016) Independent object tracking from video using the contour information in HSV color space, Indian. J Sci Technol 9(S(1)):108. https://doi.org/10.17485/ijst/2016/v9iS(1)/109907
16. Guan S (2018) Fabric defect delaminating detection based on visual saliency in HSV color space. J Text Inst 109(12):1560–1573. https://doi.org/10.1080/00405000.2018.1434112
17. Kandi S (2010) Automatic defect detection and grading of Single single-color fruits using HSV (hue, saturation, value) color space. J Life Sci 4:32
18. Kamarudin ND, Ooi CY, Kawanabe T, Mi X (2016) Tongue's substance and coating recognition analysis using HSV color threshold in tongue diagnosis. In: First International Workshop on Pattern Recognition, vol 10011. SPIE, pp 109–113. https://doi.org/10.1117/12.2242404
19. Smith S, Weller SK (2015) HSV-I and the cellular DNA damage response. Future Virol 10(4):383–397. https://doi.org/10.2217/fvl.15.18
20. Narkhede PR, Gokhale AV Color particle filter based object tracking using frame segmentation in CIELab and HSV color spaces. In: 2015 International Conference on Communications and Signal Processing (ICCSP). IEEE, pp 0804–0808. https://doi.org/10.1109/ICCSP.2015.732260
21. Truong MTN, Kim S (2017) Parallel implementation of color-based particle filter for object tracking in embedded systems. Hum Cent Comput Inf Sci 7:2. https://doi.org/10.1186/s13673-016-0082-1
22. Wang X, Jia X, Jiang C, Sanxin Jiang A (2022) Wafer surface defect detection method built on generic object detection network.

Digit Signal Process 130:103718. https://doi.org/10.1016/j.dsp.2022.103718
23. Li WC, Lin YT, Jeng JJ, Chang CL (2014) Deposition uniformity inspection in IC wafer surface. J Phys Conf Ser 483:012022 14th International Conference on Metrology and Properties of Engineering Surfaces (Met & Props 2013) 17–21 June 2013, Taipei, Taiwan
24. Ma Y, Wang F, Xie Q, Hong L, Mellmann J, Sun Y, Gao SW, Singh S, Venkatachalam P, Word J (2019) Machine learning based wafer defect detection. In: Design-Process-Technology Co-optimization for Manufacturability XIII, vol 10962. https://doi.org/10.1117/12.2513232
25. Dangayach S, Lianto P, Mishra SS (2020) Redistribution layer defect classification using computer vision techniques and machine learning. In: 2020 IEEE 22nd Electronics Packaging Technology Conference (EPTC). IEEE, Singapore, Singapore, pp 237–241. https://doi.org/10.1109/EPTC50525.2020.9315117
26. Kim JG, Yoo WS, Jang YS, Lee WJ, Yeo IG (2022) Identification of polytype and estimation of carrier concentration of silicon carbide wafers by analysis of apparent color using image processing software. ECS J Solid State Sci Technol 11(6):064003. https://doi.org/10.1149/2162-8777/ac760e
27. Al-Zubeidi A, McCarthy LA, Rafiei-Miandashti A, Heiderscheit TS, Link S (2021) Single-particle scattering spectroscopy: fundamentals and applications. Nanophotonics 10:1621–1655. https://doi.org/10.1515/nanoph-2020-0639
28. Lee H, Lee H, Jeong H, Choi S, Lee Y, Jeong M, Jeong H (2012) Macroscopic and microscopic investigation on chemical mechanical polishing of sapphire wafer. J Nanosci Nanotechnol 12:1256–1259. https://doi.org/10.1166/jnn.2012.4679
29. Gelenbe E, Koçak T, Wang R (2004) Wafer surface reconstruction from top–down scanning electron microscope images. Microelectron Eng 75:216–233. https://doi.org/10.1016/j.mee.2004.05.006
30. Takahashi S, Kudo R, Usuki S, Takamasu K (2011) Super resolution optical measurements of nanodefects on Si wafer surface using infrared standing evanescent wave. CIRP Annals 60(1):523–526. https://doi.org/10.1016/j.cirp.2011.03.053
31. Okamoto A, Kuniyasu H, Hattori T (2006) Detection of 30–40-nm particles on bulk-silicon and SOI wafers using deep UV laser scattering. IEEE Trans Semicond Manuf 19(4):372–380. https://doi.org/10.1109/TSM.2006.884600
32. Shankar NG, Zhong ZW (2005) Defect detection on semiconductor wafer surfaces. Microelectron Eng 77:337–346. https://doi.org/10.1016/j.mee.2004.12.003
33. Morris T (2016) Image processing with MATLAB, vol 14. Supporting Material for COMP27112